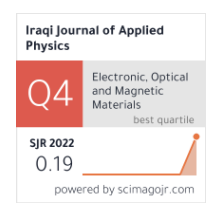
Dhulfiqar S. Mutashar ^{1,2} Wasan R. Saleh ¹ Ilham A. Khalaf ³

Department of Physics, College of Science, University of Baghdad, Baghdad, IRAQ Department of Applied Sciences, University of Technology, Baghdad, IRAQ Corporation of Research and Industrial Development, Baghdad, IRAQ



Structural and Electrochemical Characterization of ITO Electrode Modified by f-MWCNT/graphene/polypyrrole Nanocomposite Decorated by Gold Nanoparticles

There is currently a pressing need to create an electro-analytical approach capable of detecting and monitoring genosensors in a highly sensitive, specific, and selective way. In this work, Functionalized Multiwall Carbon Nanotubes. Polypyrrole, gold Graphene, and nanoparticles nanocomposite (f-MWCNTs-GR-PPv-AuNP) were effectively deposited on the surface of the ITO electrode using a drop-casting process to modify it. The structural, morphological, and optical analysis of the modified ITO electrodes was carried out at room temperature using X-ray diffraction (XRD), field emission scanning electron microscopy (FE-SEM) images, atomic force microscopy (AFM) and Fourier transform infrared (FTIR) spectra. Cyclic voltammetry (CV) and electrochemical impedance spectroscopy (EIS) were used to assess the electroanalytical performance of the electrodes after modification. The results showed that using AuNPs and PPy for modification of ITO/f-MWCNTs-GR electrode surfaces is conducive to augmenting the electrochemical performances of the electrodes. ITO/f-MWCNTs-GR showed better results in terms of higher electroactive area formation after modification with PPy and AuNPs. This work aims to figure out how to develop electrochemical biosensors for improved genosensor monitoring.

Keywords: Electrochemical characterization; Nanostructures; Nanocomposite; Polypyrrole Received: 04 November 2023; Revised: 05 December 2023; Accepted: 12 December 2023

1. Introduction

In recent years, considerable attention has been given by numerous researchers to the advancement of carbonaceous materials such as graphene (GR) [1], carbon nanotubes (CNTs) [2], and other materials combined with semiconductors, metal compounds [3], and conductive polymers [4]. Various studies have been conducted to explore their potential in optoelectronic [5], photocatalytic [6], and supercapacitor applications [7].

Nanocomposites made of conducting polypyrrole (PPy) and nanoparticles have gotten a lot of interest [8, 9]. These nanocomposites have been proposed as ideal protective layers for biosensors and for facilitating charge transfer. When compared to insulating polymer nanocomposites, conducting polymers unparalleled exhibit electroactive properties, effectively connecting metal nanoparticles (NPs) within the nanocomposite matrix. As a result, the synthesis of novel nanocomposites based on metal nanoparticles and conducting polymers holds great promise for exciting advancements nanotechnological applications [10-13].

Gold nanoparticles (AuNPs) are frequently utilized in the fabrication of electrochemical sensors because of their elevated catalytic efficacy,

exceptional biocompatibility, and expeditious electron transfer velocity [14,15]. The integration of MWCNTs-GR hybrid nanocomposite with Au nanoparticles not only prevents the aggregation of Au nanoparticles but also augments the electro-catalytic activity of the electrode [16].

The electrochemical approach is one of the most widely used analytical procedures because to its low cost, ease of production, high sensitivity, and suitability for real-time sample analysis which made it an important tool in biosensor applications [17-20].

Several systems for detecting genetic diseases have been developed and are primarily based on enzyme-linked immunosorbent assays (ELISA), fluorescence, and electrochemical technologies. In order to develop sensors that possess user-friendly characteristics and are accessible to individuals of all backgrounds and capabilities [21], therefore, the goal of this work is to demonstrate how incorporating gold nanoparticles (AuNPs) and polypyrrole (PPy) into Functionalized Multiwall Carbon Nanotubes (f-MWCNTs) and graphene might offer a viable strategy electrochemical to improve the characteristics of those nanoparticle-based ITO electrodes.

2. Experimental Work

The used material in this work are, functionalized MWCNTs (f-MWCNTs) with 5.3-5.85% OH supplied by Nanostructured and Amorphous Materials, Inc. (f-MWCNTs) (having an outer diameter of 8 nm, a length of 0.5-2 nm and a purity of >95.1%). Graphene Nanoplatelets (GR) with purity of >99.5+ %, 28 nm supplied by US Research Nanomaterials, Inc. Gold nanoparticles (AuNPs) with purity of >99.97% APS: 28nm, bulk density ~ 0.85 g/m³, supplied by US Research Nanomaterials, Inc. Dimethyl sulfoxide (DMSO) solution of formula (CH₃)₂SO with the molecular weight 78.14 (g/mol), purity 99.6% supplied by ALPHA CHEMIKA, India. While N, N Dimethylformamide (DMF) solution of formula C_2H_7NO with the molecular weight 73.08(g/mol), density 0.944 gm/ml (at 25 °C) used to prepare f-MWCNTs -PPy-AuNPs suspension, was supplied by Biosolve, USA Company. For electrolyte solution, Potassium ferrocyanide (Fe(CN)₆]^{-3/-4})of purity 99 % and Potassium chloride (KCl) of purity 99 % both from Sigma- Aldrich. The chemicals were utilized as received, without further purification.

For the preparation of f-MWCNTs-GR-AuNPs suspension, 2 mg of f-MWCNTs and 2 mg of GR were mixed in 2.0 mL of DMF and sonicated for 15 min. by a sonicated probe, then 2 µg of AuNPs were added to the suspension and sonicated again for 15 min. for a homogenous distribution. Polypyrrole conductive polymer is prepared through easy and low-cost in-situ chemical oxidative polymerization, as described in [22,23]. The PPy solution is immediately injected into the (f-MWCNTs-GR-AuNPs) synthesis suspension using a microsyringe. The breaking up of f-MWCNTs aggregation and generating a small network. This is accomplished by sonicating the mixture for 20 min. using an ultrasonic probe. Figure (1) shows the schematic diagram of the synthesis steps.

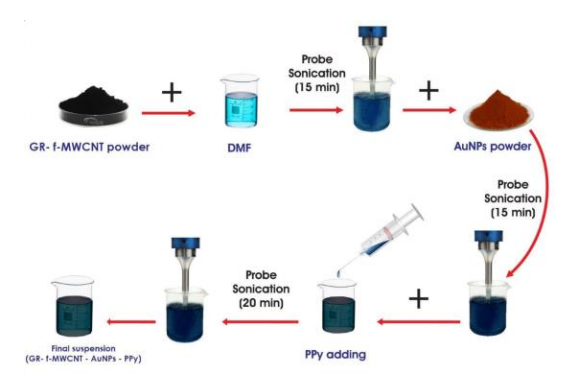


Fig. (1) Schematic diagram of the (f-MWCNTs-PPy -AuNPs) composite synthesis steps

An ITO-conductive glass with an area of $1cm^2$ was used as a working electrode (WE) for the electrochemical system. To modify this electrode, a micropipette was used to drop 7μ L of the suspension onto the ITO surface with area $1cm^2$. The (ITO/f-MWCNTs-GR-PPy-AuNPs) modified electrode was

successfully constructed after drying at room temperature. The schematic representation of the constructed, modified electrode is shown in Fig. (2).



Fig. (2) Schematic diagram of the proposed ITO electrode modification process

3. Results and discussion

The XRD pattern of the generated f-MWCNT-G-AuNPs-PPy composite is shown in Fig. (3). The XRD pattern displays a wide peak at 2θ =23.5°, indicating that PPy is amorphous [24]. Carbon has a prominent peak in the spectra of f-WMCNTs at 2θ =26.6° Miller indices (002) (JCPDS file 96-1061). Diffraction peaks for AuNPs were detected at 2θ =37°, 2θ =63.42°, and 2θ =78.48° corresponding to (111), (200), and (311) respectively (JCPDS file 89-3697). As a consequence, it was hypothesized that - stacking between the PPy chains and graphene planes occurs [25].

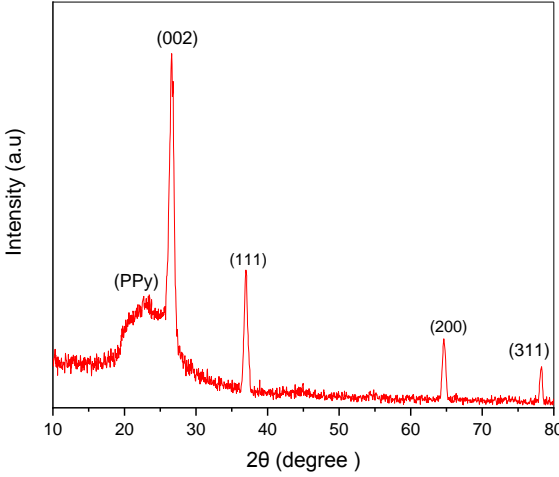
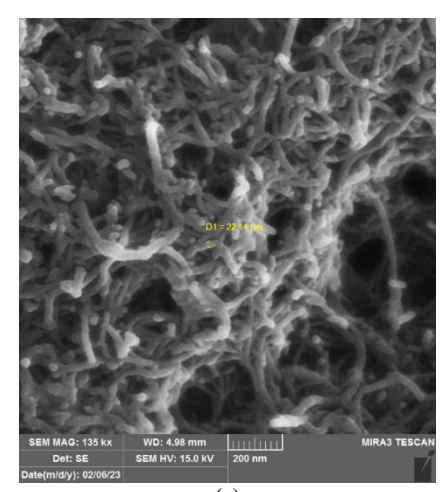
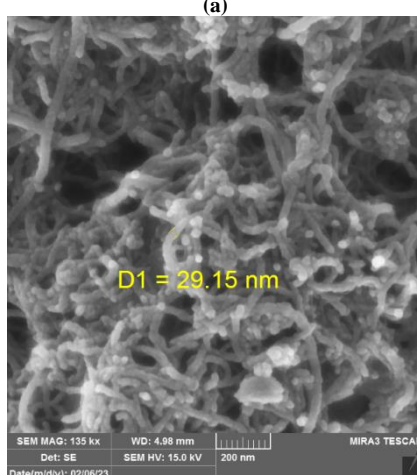


Fig. (3) XRD pattern of f-MWCTs-G-AuNPs-PPy

Field-emission scanning electron microscopy (FE-SEM) was used to examine the surface morphologies of modified ITO electrodes. Figure (4a) shows a homogenous layer of f-MWCNTs -GR nanocomposite at the surface of the modified ITO electrode. f-MWCNTs -GR nanocomposite along with well-dispersed AuNPs is observed as shown in Fig. (4b). Figure (4c) depicts a thick layer of PPy covering the f-MWCNTs-GR-AuNPs nanocomposite, this might be because more pyrrole was present during the in-situ polymerization process, which promotes the formation of PPy on the

surface of the f-MWCNTs-GR-AuNPs, resulting in a thick coating.





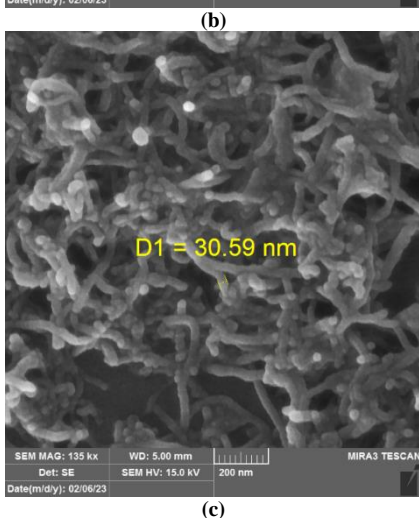


Fig. (4) SEM images of (a): f-MWCNTs-GR, (b) f-MWCNTs-GR-AuNPs and (c) f-MWCNTs-GR-AuNPs nanocomposite

AFM images in Fig. (5) revealed the existence of nanoparticles with a homogeneous distribution on the ITO surface with some regions of agglomeration. The surface roughness (Sa) value for f-MWCNTs-GR-AuNPs-PPy was 120 nm, Root Mean Square 152 nm and Ten-point height 474 nm. Furthermore, various aggregation regions were appeared in the images.

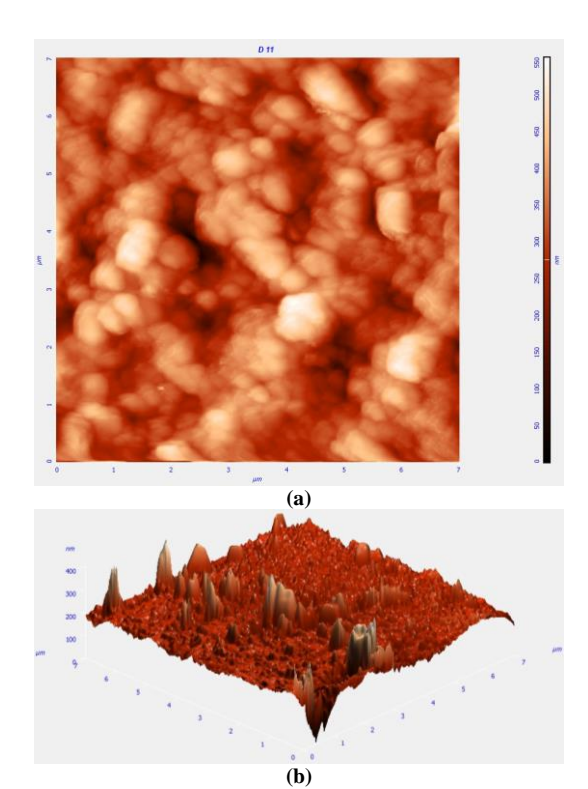


Fig. (5) 2D and 3D AFM images of f-MWCNTs-GR-AuNPs-PPy $\,$

The FTIR spectra of the generated suspension were measured in the 500-4000 cm^{-1} range using a Thermo Nicolet Avatar 360 FT-IR Spectrometer. Figure (6) depicts the FTIR spectra of different electrodes. Peaks in curve PPy at 1027 cm⁻¹, $1311 \, cm^{-1}$ and $1433 \, cm^{-1}$ may be attributed to C-H (alkene bending), C=C deformation vibrations and C-N stretching, respectively. This band is associated to C–C stretching vibration at $1256 cm^{-1}$. The tiny peaks observed in all curves at $1671 cm^{-1}$ are due to the C=O bond and are most likely due to PPy, GR and f-MWCNTs impurities. Furthermore, the faint peaks at 2935 cm⁻¹ are caused by C-N vibration. The stretching vibration of the O-H carbonyl and hydroxyl functional groups is responsible for the broad peak at $3500 cm^{-1}$. This results in good agreement with the results of Alagappan et al [26].

In this study, voltammetric measurements were performed with an IRASO1 PGS-10 potentiostat/galvanostat and LMS-27 software. Electrochemical tests used a 200mL electrochemical cell with a modified ITO working electrode (WE), Ag/AgCl reference electrode (RE) and platinum wire counter electrode (CE). EIS studies were performed using a PGS-18 potentiostat.

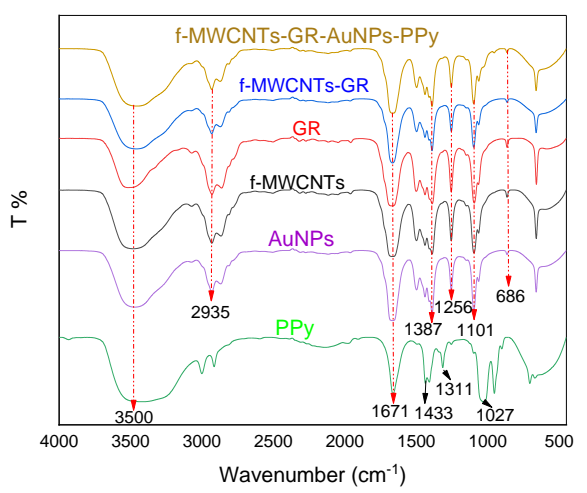


Fig. (6) FTIR spectra of PPy, GR, f-MWCNTs, AuNPs, f-MWCNTs-AuNPs, and f-MWCNTs-GR-PPy -AuNPs composite

Figure (7) shows the CV of the modified electrodes versus the ITO electrode in 10 mM $[\text{Fe}(CN)_6]^{-3/-4}$ in 0.1 M KCl solution, and (-0.5–1.2) V potential range. The electrochemical responses of samples were studied using CV at a scan rate 100 mV/s. Figure (7) revealed with the f-MWCNTs-GR nanocomposites sample have a stronger current response and a larger CV loop area than f-MWCNTs and graphene samples scanned at the same scan rate.

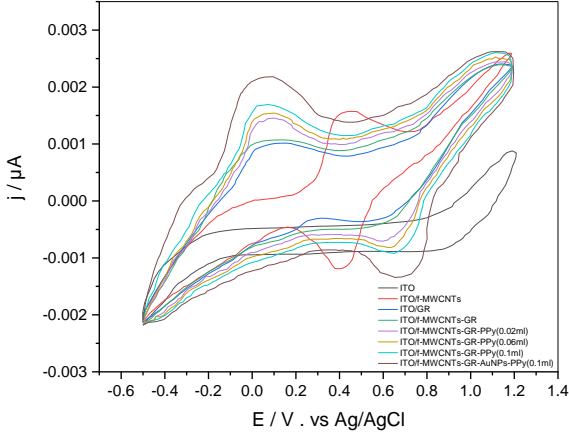


Fig. (7) Cyclic voltammograms for ITO, f-MWCNTs, GR, f-MWCNTs-GR, f-MWCNTs-GR-PPy(0.02mL), f-MWCNTs-GR-PPy(0.06mL), f-MWCNTs-GR-PPy(0.1mL), and f-MWCNTs-GR-AuNPs-PPy (0.1mL)

The PPy concentration was optimized by examining the cyclic voltammograms (CVs) of various modified ITO electrodes. Figure 7, appears that with the increasing to the pyrrole concentration from 0.02 mL to 0.1 mL raised the anodic peak current from $0.00107 \mu A$ to $0.00171 \mu A$ at a potential of 0.9 V. The observed phenomenon may be attributed to a heightened electrode conductivity which is a result of the penetration of PPy into the layers of the f-MWCNTs-GR nanocomposite, coupled with an increase in space within the layers of the nanocomposite. PPy was effectively absorbed

electrostatically onto the GR layer [27]. Subsequently, PPy was intercalated between the f-MWCNTs-GR layers forming a sandwiched structure. The optimal quantity of pyrrole was determined to be 0.1mL. Existing of PPy increased the electrode conductivity by boosting background current due to its superior electrical characteristics [28]. The increased electroactive surface area provided by the PPy-containing electrode causes an increase in current levels.

The incorporation of AuNPs was observed to have caused a surge in the anodic peak current, as evidenced. This phenomenon was attributed to the agglomeration of AuNPs, which consequently led to an enlargement in the size of the particles. [29].

In Electrochemical Impedance Spectroscopy (EIS), data collected from measurements are fitted to an equivalent electrical circuit model specified circuit to identify its characteristics. An equivalent electrical circuit was built employing ZSimpWin software using the impedance spectra.

Figure (8) shows the fitting operations were carried out using the circuit description code $R_s(\text{Cdl}(R_{ct}W))$, where R_s represents the solution resistance, Cdl represents the double layer capacitance, R_{ct} represents the charge-transfer resistance, and W represents the Warburg impedance. At high frequencies, the semicircle is connected to R_{ct} , while at very low frequencies, the Warburg impedance is related to analyte diffusion from solution to working electrode surface.

The electron transport capacities of bare ITO electrodes and modified ITO electrodes were investigated using electrochemical impedance spectroscopy (EIS) as shown in Fig. (9). Semicircles followed by diffusion tails were seen on both the ITO bare and modified ITO electrodes, which are typical features of the diffusion process. The (R_{ct}) is a vital parameter that significantly affects electrochemical phenomena transpiring at the electrode surface. It is analogous to the semicircle diameter of the EIS and can be assessed through the semicircle diameter of the Nyquist plots [30]. For the bare ITO, ITO/f-MWCNTs, ITO/GR, ITO/f-MWCNTs-GR, ITO/f-MWCNTs-GR-PPy(0.02mL), ITO/f-MWCNTs-GR-ITO/f-MWCNTs-GR-PPy(0.1mL) PPy(0.04mL),ITO/f-MWCNTs-GR-AuNPs-PPy(0.1mL) modified electrodes, approximate diameter values of 79, 4, 42, 40, 38, 36, 25, and 18 k Ω (R_{ct}) were determined, respectively. The alteration of electrodes with ITO/f-MWCNTs-GR-AuNPs-PPy led the decrease in resistance that means decrease in value of R_{ct} , this is attributed to the properties of the materials used such as current responsiveness, charge mobility, Higher conductivity, quick charge/discharge ability, and high power density. The best result obtained by relying on the value of R_{ct} is when electrode modified with ITO/f-MWCNTs-GR-AuNPs-PPy (0.1mL). It is believed that this case is the most optimal in terms of electrochemical catalytic

integration associated with an increase in electrode electron transport.

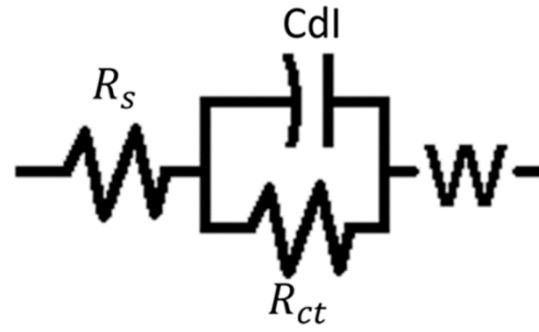


Fig. (8) Equivalent electrical circuit used in EIS fitting data for electrodes

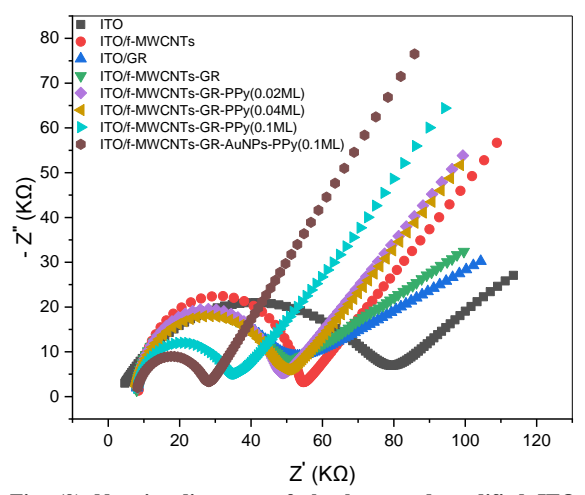


Fig. (9) Nyquist diagrams of the bare and modified ITO electrode before and after modification

4. Conclusions

In this work, physical and electrochemical characterization demonstrated that the quantity of f-MWCNTs-GR-AuNPs-PPy(0.1mL) was optimal for application as a sensor. Due to the remarkable conductivity and high surface area of f-MWCNTs-GR and AuNPs, integrating the nanocomposite onto the ITO has enhanced the surface roughness, ITO surface area, and conductivity characteristics. Based on the findings, it is discernible that the altered ITO electrode exhibits remarkable potential for employment in bio-applications such as genosensors owing to its exceptional sensitivity, expansive linear range, negligible detection limit and commendable repeatability.

Acknowledgment

The authors would like to thank the staff of the laboratory of Laser and Electro-Optics, Department of Physics, College of Science, University of Baghdad, and everyone who contributed to the success of this work

References

[1] S. Bao et al., "Immobilization of Zinc Oxide Nanoparticles on Graphene Sheets for Lithium

- Ion Storage and Electromagnetic Microwave Absorption", *Mater. Chem. Phys.*, 245 (2020) 122766.
- [2] A.G. Enad, E.T. Abdullah and M.Gh. Hamed, "Study the Electrical Properties of Carbon Nanotubes/Polyaniline Nanocomposites", *J. Phys.: Conf. Ser.*, 1178 (2019) 012032.
- [3] S.H. Kim, J.Y. Lee and Y.S. Yoon, "Effect of composite structure on capacity instability of SnO₂-Coated multiwalled carbon nanotube composite anode", *J. Alloys Comp.*, 742 (2018) 542-548.
- [4] F.M. Ahmed, S.M. Hassan and M.I. Kamil, "The DC Electrical Conductivity of Prepared Pure Polypyrrole and Polypyrrole/Graphene (PPy/GN) Nanocomposite by *in-situ* Polymerization", *Iraqi J. Phys.*, 18(44) (2020) 50-61.
- [5] P. Das et al., "Improved Charge Transport Properties of Graphene Incorporated Tin Oxide Based Schottky Diode over Pure One", *J. Phys. Chem. Solids*, 148 (2021) 109706.
- [6] S. Gayathri et al., "Synthesis of ZnO Decorated Graphene Nanocomposite for Enhanced Photocatalytic Properties", *J. Appl. Phys.*, 115(1) (2014) 173504.
- [7] M. Fu et al., "One-Step Preparation of One Dimensional Nickel Ferrites/Graphene Composites for Supercapacitor Electrode with Excellent Cycling Stability", *J. Power Sources*, 396 (2018) 41–48.
- [8] S.M. Omran, E.T. Abdullah and O.A. Al-Zuhairi, "Polyvinylpyrrolidone/Multi-Walled Carbon Nanotubes/Graphene Nanocomposite as Gas Sensor", *Iraqi J. Sci.*, 63(9) (2022) 3719-3726.
- [9] M.K. Jawad et al., "Preparation and Characterization of Poly (1-vinylpyrroli done-co-vinyl acetate)/Poly (methyl methacrylate) Polymer Electrolyte based on TPAI and KI", *Adv. Phys. Theor. Appl.*, 29 (2014) 14-22.
- [10] K. Xue et al., "A Novel Amperometric Glucose Biosensor Based on Ternary Gold Nanoparticles/Polypyrrole/Reduced Graphene Oxide Nanocomposite", *Sens. Actuat. B: Chem.*, 203 (2014) 412–416.
- [11] F. Wang, Z. Lihua and J. Zhang, "Electrochemical Sensor for Levofloxacin Based on Molecularly Imprinted Polypyrrole—Graphene—Gold Nanoparticles Modified Electrode", Sens. Actuat. B: Chem., 192 (2014) 642–647.
- [12] S.M. Abdalcareem and M.K. Jawad, "Effect of cation size on electrochemical properties of polymer electrolyte", *Iraqi J. Phys.*, 17(42) (2019) 76-84.
- [13] C. Ye et al., "Study on the Properties and Reaction Mechanism of Polypyrrole@norfloxacin Molecularly Imprinted Electrochemical Sensor Based on

- Three-Dimensional Cofe-Mofs/Aunps", *Electrochimica Acta*, 379 (2021) 138174.
- [14] S.S. Nair, S.A. John and T. Sagara, "Simultaneous Determination of Paracetamol and Ascorbic Acid Using Tetraoctylammonium Bromide Capped Gold Nanoparticles Immobilized on 1,6-Hexanedithiol Modified Au Electrode", *Electrochimica Acta*, 54(27) (2009) 6837–6843.
- [15] B. Wang et al., "Enhanced Electrocatalytic Activity of Graphene-Gold Nanoparticles Hybrids for Peroxynitrite Electrochemical Detection on Hemin-Based Electrode", *Bioelectrochem.*, 118 (2017) 75–82.
- [16] Z. Wang et al., "Simultaneous and Selective Measurement of Dopamine and Uric Acid Using Glassy Carbon Electrodes Modified with a Complex of Gold Nanoparticles and Multiwall Carbon Nanotubes", Sens. Actuat. B: Chem., 255 (2018) 2069–2077.
- [17] S.Z. Mousavisani et al., "Label-Free DNA Sensor Based on Diazonium Immobilisation for Detection of DNA Damage in Breast Cancer 1 Gene", Sens. Actuat. B: Chem., 264 (2018) 59–66.
- [18] T. Tian et al., "Paper-Based Biosensor for Noninvasive Detection of Epidermal Growth Factor Receptor Mutations in Non-Small Cell Lung Cancer Patients", *Sens. Actuat. B: Chem.*, 251 (2017) 440–445.
- [19] F. Otero and E. Magner, "Biosensors Recent Advances and Future Challenges in Electrode Materials", *Sensors*, 20(12) (2020) 3561.
- [20] M.A. Al-Azzawi and W.R. Saleh, "Detection of Zn water pollution by a biosensor based on alkaloids derived from Iraqi Catharanthus roseus", *Accepted for publication by Iraqi J. Sci.*
- [21] J. Xu et al., "Recent advances in disease diagnosis based on electrochemical-optical dual-mode detection method", *Talanta*, 253 (2023) 124037.
- [22] A.Y. Taradh and W.R. Saleh, "Fabrication and Characterization of Functionalized Multi-Wall

- Carbon Nanotubes Flexible Network Modified by a Layer of Polypyrrole Conductive Polymer and Metallic Nanoparticles", *Nano Hybrid. Compos.*, 36 (2022) 21–33.
- [23] F.M. Ahmed and S.M. Hassan, "Optical and A.C. Electrical Properties for Polypyrrole and Polypyrrole/Graphene (Ppy/GN) Nanocomposites", *Iraqi J. Phys.*, 19(51) (2021) 72–78.
- [24] A. Srinivasan, P. Ranjani and N. Rajendran, "Electrochemical Polymerization of Pyrrole over AZ31 MG Alloy for Biomedical Applications", *Electrochimica Acta*, 88 (2013) 310-321.
- [25] J. Zhang et al., "Graphene–Hollow PPy Sphere 3D-Nanoarchitecture with Enhanced Electrochemical Performance", *Nanoscale*, 5(7) (2013) 3052.
- [26] M. Alagappan et al., "Development of Cholesterol Biosensor Using Au Nanoparticles Decorated F-MWCNT Covered with Polypyrrole Network", *Arabian J. Chem.*, 13(1) (2020) 2001–2010.
- [27] S.K. Hussain, B. Dudem and J.S. Yu, "Enhanced Electrochemical Performance via PPy Encapsulated 3D Flower-like Bismuth Molybdate Nanoplates for High-Performance Supercapacitors", *Appl. Surf. Sci.*, 478 (2019) 846-856.
- [28] M.E. Roberts et al., "High Specific Capacitance Conducting Polymer Supercapacitor Electrodes Based on Poly(Tris (Thiophenylphenyl)Amine)", *J. Mater. Chem.*, 19(38) (2009) 6977.
- [29] O. Vajdle et al., "Voltammetric Behavior of Doxorubicin at a Renewable Silver-Amalgam Film Electrode and Its Determination in Human Urine", *Electrochimica Acta*, 132 (2014) 49-57.
- [30] R. Hajian, Z. Tayebi and N. Shams, "Fabrication of an Electrochemical Sensor for Determination of Doxorubicin in Human Plasma and Its Interaction with DNA", *J. Pharmaceut. Anal.*, 7(1) (2017) 27-33.